MolecularMedicine

Methylene Blue Reduces Acute Cerebral Ischemic Injury via the Induction of Mitophagy

Yao Di,[1] Yun-Ling He,[1] Tong Zhao,[1] Xin Huang,[1] Kui-Wu Wu,[1] Shu-Hong Liu,[1] Yong-Qi Zhao,[1] Ming Fan,[1,2,3] Li-Ying Wu,[1] and Ling-Ling Zhu[1,2]

[1]Department of Cognitive Science, Beijing Institute of Basic Medical Sciences, Beijing, People's Republic of China; [2]Co-innovation Center of Neuroregeneration, Nantong University, Nantong, People's Republic of China; and [3]Beijing Institute for Brain Disorders, Beijing, People's Republic of China

The treatment of stroke is limited by a short therapeutic window and a lack of effective clinical drugs. Methylene blue (MB) has been used in laboratories and clinics since the 1890s. Few studies have reported the neuroprotective role of MB in cerebral ischemia-reperfusion injury. However, whether and how MB protects against acute cerebral ischemia (ACI) injury was unclear. In this study, we investigated the effect of MB on this injury and revealed that MB protected against ACI injury by augmenting mitophagy. Using a rat middle cerebral artery occlusion (MCAO) model, we demonstrated that MB improved neurological function and reduced the infarct volume and necrosis after ACI injury. These improvements depended on the effect of MB on mitochondrial structure and function. ACI caused the disorder and disintegration of mitochondrial structure, while MB ameliorated the destruction of mitochondria. In addition, mitophagy was inhibited at 24 h after stroke and MB augmented mitophagy. In an oxygen-glucose deprivation (OGD) model in vitro, we further revealed that the elevation of mitochondrial membrane potential (MMP) by MB under OGD conditions mediated the augmented mitophagy. In contrast, exacerbating the decline of MMP during OGD abolished the MB-induced activation of mitophagy. Taken together, MB promotes mitophagy by maintaining the MMP at a relatively high level, which contributes to a decrease in necrosis and an improvement in neurological function, thereby protecting against ACI injury.

Online address: http://www.molmed.org
doi: 10.2119/molmed.2015.00038

INTRODUCTION

Stroke is a primary cause of disability and death worldwide. The treatment of stroke is constrained by a therapeutic window consisting of a few hours, and effective drugs for the treatment of stroke are extremely scarce. Methylene blue (MB) has been demonstrated to perform diverse biological functions and has been used for various medical applications (1). MB readily crosses the blood–brain barrier and accumulates in the mitochondrial matrix (2,3); therefore, its biological functions primarily involve improving mitochondrial functions, such as enhancing cytochrome c oxidase activity (4), oxygen consumption (5, 6) and ATP production (7) and reducing reactive oxygen species (ROS) generation (8). Clinically, MB has been approved by the FDA for methemoglobinemia and as an antidote to cyanide poisoning (9,10). A few studies have shown that MB reduces cerebral ischemia-reperfusion injury (11–13). In fact, fewer than 5% of patients with ischemic stroke can obtain thrombolytic treatment in the therapeutic window (14). That is, more than 95% of patients suffer permanent cerebral ischemia due to not receiving reperfusion in time. Acute cerebral ischemia (ACI) is one of the most common cerebral vascular diseases and here refers to the process whereby artery blockage causes brain tissue ischemia without reperfusion, resulting in brain dysfunction. The importance and necessity of ACI treatment lies in early intervention, without considering reperfusion or not, to reduce the mortality and disability. Therefore, the research and development of neuroprotective drugs for the treatment of acute ischemic stroke is clinically significant. Here, we demonstrate for the first time that MB attenuates ACI injury and that its protective effect is related to the induction of mitophagy.

Mitochondria are the principal target of ischemic injury (15). Ischemia generally

Address correspondence to Ling-Ling Zhu, Li-Ying Wu, or Ming Fan, Department of Cognitive Science, Beijing Institute of Basic Medical Sciences, 27 Taiping Road, Beijing, 100850, P.R. China. Phone: +86-10-66931315 (LLZ), +86-10-66931316 (LYW), +86-10-66932333 (MF); Fax: +86-10-68213039 (LLZ, LYW, MF) ; E-mail: linglingzhu@hotmail.com (LLZ), liyingwu_china@163.com (LYW), fanmingchina@126.com (MF).

The Feinstein Institute for Medical Research
Empowering Imagination. Pioneering Discovery.®

North Shore LIJ

leads to mitochondrial dysfunction (16,17). Dysfunctional mitochondria can be selectively eliminated via mitophagy (18–20). In this process, damaged mitochondria are enveloped by double-membrane structures known as autophagosomes, which are then delivered to lysosomes for degradation (21–23). Thus, mitophagy plays a crucial role in controlling the quality of mitochondria by preventing the generation of ROS by dysfunctional mitochondria (24,25). Deficiency in mitophagy is associated with neurodegenerative diseases such as Parkinson's disease (26,27), Alzheimer's disease (28,29) and Huntington's disease (30). Stroke is another type of neurodegenerative disease. However, whether mitophagy is involved in the pathogenesis of stroke and whether MB interrupts this process remain unclear.

Using a rat middle cerebral artery occlusion (MCAO) model of stroke, we have demonstrated that mitophagy is induced in the early stage of stroke but is inhibited shortly thereafter (data not shown). In this study, we showed that 24 h of ischemia suppressed mitophagic activity but that MB treatment rescued it. We confirmed this effect of MB using an oxygen-glucose deprivation (OGD) model *in vitro* and identified that the protection conferred by MB during OGD was abolished due to the inhibition of mitophagy. As mitophagy is directly induced by the loss of mitochondrial membrane potential (MMP) (27,31–33), we further explored whether the effect of MB on mitophagy was mediated by the regulation of MMP. We found that the MMP dramatically declined after cells were exposed to OGD, whereas MB attenuated this decline. Moreover, we verified that the relatively high MMP maintained by MB during OGD contributed to the activation of mitophagy.

MATERIALS AND METHODS

Middle Cerebral Artery Occlusion and Methylene Blue Treatment

Adult male Sprague Dawley rats were purchased from Vital River Laboratories (Beijing, China). Focal ischemia was induced via right MCAO as described previously (34). Briefly, focal cerebral ischemia was induced by inserting a 4-0 nylon monofilament through the right internal carotid artery. Different doses (1, 5 or 10 mg/kg) of MB or vehicle (normal saline) were intraperitoneally (IP) injected immediately after occlusion. The animal protocol was approved by the Institutional Animal Care and Use Committee of the Academy of Military Medical Science, and all measures were taken to reduce animal numbers and suffering.

Neurological Deficit Score Assessment

Total neurological deficit score. This test, which consisted of two sections, was conducted at 24 h after MCAO with or without MB treatment: (1) the postural reflex test was performed to evaluate upper body posture while the rat was suspended by the tail, and (2) the forelimb placing test was performed to examine sensor motor integration in forelimb placing responses to visual, tactile and proprioceptive stimuli. The total neurological deficit score was graded on a scale from 0 (normal score) to 12 (maximal score) (35).

Grid-walking test. Each animal was placed individually on a grid with an area of 110 × 10 × 100 cm (length × width × height) containing 9-cm^2 wire mesh and were allowed to freely walk for 5 min. During this 5-min period, the total number of foot faults by the ipsilateral forelimb was counted. If the rat was resting with the grid at the level of the wrist, this positioning was also considered as a fault. If the rat was not able to step for 5 min, the maximal score of 15 was assigned (36).

Infarct Volume Analysis

The rats were anesthetized and euthanized 3, 6, 9, 12 or 24 h after MCAO. The brains were rapidly removed and were placed in a rat mold to generate 2-mm coronal sections. The sections were stained with 1% (w/v) 2,3,5-triphenyltetrazolium chloride (TTC) solution at room temperature for 30 min and then fixed in 4% paraformaldehyde. The infarct size was measured and analyzed using ImageJ software. To compensate for the effect of brain edema, the corrected infarct volume was calculated as described previously: corrected infarct area = left hemisphere area – (right hemisphere area – infarct area) (37).

Hematoxylin and Eosin Staining

The brain tissues from the rats were embedded in paraffin and 6-μm-thick serial coronal sections were generated and mounted on slides. The sections were stained using hematoxylin and eosin (H&E) according to a previously described standard protocol (38).

Transmission Electron Microscopic Examination

The tissue samples were handled as reported previously (39). Briefly, brain section was quickly cut into 1 mm cubes, immersion-fixed with 2.5% glutaraldehyde in 0.1 mol/L phosphate buffer (pH 7.4) overnight at 4°C and fixed in 1% buffered osmium tetroxide. Specimens were dehydrated through a graded ethanol series and embedded in epoxy resin. For mitochondrial structure analysis, we used a grading system to perform a quantitative evaluation. The mitochondria scoring parameters were as follows (40):

0: Normal mitochondrion.
1: Normal mitochondrion but lacking granular deposits.
2: Loss of matrix granules and clarification of the matrix without disruption of cristae.
3: Loss of matrix granules, uniform clarification of the matrix and disruption of cristae.
4: Loss of matrix granules, uniform disruption of cristae, and loss of mitochondrial membrane integrity.

The samples were visualized and photographed using a transmission electron microscope (TEM) at 80 kV.

FJB and TUNEL Labeling

Cell necrosis was determined via Fluoro-Jade B (FJB; Millipore, Billerica, MA, USA) labeling and terminal deoxynucleotidyl transferase-mediated bi-

otinylated UTP nick-end labeling (TUNEL). At 24 h after MCAO, the rats were anesthetized and transcardially perfused with saline followed by cold 4% paraformaldehyde (PFA) solution. The brains were rapidly removed and cryoprotected in 30% sucrose. FJB and TUNEL labeling were performed using *in situ* death detection kits as described previously (41). Fluorescence signals were visualized via fluorescence microscopy.

Cell Culture and Oxygen-Glucose Deprivation

A hypoxia-sensitive neuron-like PC12 cell line was used to simulate cerebral ischemia in an OGD model. The cells were cultured at 37°C in RPMI 1640 medium supplemented with 10% fetal bovine serum (FBS), 100 U/mL penicillin and 100 mg/mL streptomycin in 5% CO_2. For OGD, the cultures were placed in a hypoxic incubator containing 0.3% O_2 and a gas mixture of 95% N_2/5% CO_2, and the medium was replaced with glucose-free RPMI 1640 medium for 2 h. For treatment, MB (0.5 μmol/L) dissolved in PBS (phosphate buffered saline) or an inhibitor (3-MA, 2 mmol/L; carbonyl cyanide m-chlorophenylhydrazone (CCCP), 1 μmol/L) was added to the culture medium immediately when the cells were exposed to OGD.

Western Blot

Brain sections that included the ischemic area and corresponding regions from the contralateral hemisphere or cells were collected, and protein extracts were prepared as described previously (34). The primary antibodies used for Western blot–targeted receptor-interacting protein 1 or 3 (RIP1/RIP3), microtubule-associated protein light chain 3 (LC3), translocase of the outer membrane of mitochondrion (Tom20), Beclin1, P62 or β-actin. The signals were detected with the use of an ECL Western blot substrate (Thermo Fisher Scientific Inc., Waltham, MA, USA). Quantitative analyses were performed using the ImageJ software (NIH, Bethesda, MD, USA).

ROS Detection

The intracellular ROS levels were measured using the oxidation-sensitive fluorescent probe CM-H_2DCFDA after OGD. The cells were incubated in 10 μmol/L CM-H_2DCFDA in the dark at 37°C for 30 min and then washed with PBS. The suspended cells were analyzed via flow cytometry.

Mitochondrial Membrane Potential Assessment

The MMP was determined by using the fluorescent probe JC-1 two hours after OGD in PC12 cells according to the manufacturer's directions. The ratio of red:green fluorescence of JC-1 is dependent on the MMP. After treatment, the cells were incubated in 2.5 μmol/L JC-1 for 20 min at 37°C and then rinsed twice with PBS. Afterward, the cells were collected and analyzed via flow cytometry (42).

Statistical Analyses

The data are presented as the means ± SE. Differences between the control and experimental groups were examined via one-way analysis of variance (ANOVA). Values of $P < 0.05$ were considered to be significant. At least three independent experiments were performed for each experiment.

All supplementary materials are available online at www.molmed.org.

RESULTS

MB Attenuates the Infarct Volume and Improves Neurological Functions

To assess the effects of MB on ACI injury, SD rats were subjected to MCAO for 24 h. We found that ischemia caused massive cerebral infarction in the vehicle control (VC) group; all three doses of MB reduced the infarct volume and, among these doses, the medium dose of MB displayed the most significant effect, an approximate 50% reduction in the infarct volume (Figures 1A–B). Decreased brain damage in the MB-treated rats was accompanied by reduced neu-

rological deficit scores. The animals treated with the medium dose of MB showed attenuated injury in the impaired limb on the forelimb placing test (Figure 1C). On the grid-walking test, a clear increase in forepaw foot faults was observed at 24 h after stroke. The animals treated with the medium or high dose of MB showed a significant reduction in forepaw foot faults after stroke (Figure 1D). These data showed that MB treatment reduced the infarct volume and improved neurological functions after ACI injury.

MB Alleviates the Destruction of Brain Tissue Morphology

The morphological changes in brain tissue were detected via H&E staining at 24 h after stroke. As shown in Figure 2A, cell swelling and nuclear pyknosis were detected in the VC group; in contrast, all three doses of MB improved the histological appearance. The statistical data showed that the percentage of swelling cells was significantly reduced by MB compared with the VC (Figure 2B). The results provide further evidence that MB greatly prevented cell swelling and brain tissue destruction. Necrosis and apoptosis are the principal mechanisms of ischemic injury (43). Whether these morphological alterations are determined by the degree of necrosis or apoptosis and what role MB plays in the process both need to be clarified.

MB Decreases Necrosis Rather than Apoptosis

Using FJB and TUNEL double-fluorescence staining, we analyzed necrosis and apoptosis at 24 h after stroke. TUNEL labeling represents apoptotic cells, and FJB labeling represents degenerating cells, including apoptotic and necrotic cells (41). We observed that MB did not decrease apoptosis, but actually increased it (see Supplemental Figure 1); however, the percentage of necrotic cells, as determined by FJB labeling, excluding the TUNEL-positive cells, was significantly less in the MB treatment group than in the VC group (Figures 3A–C). At the
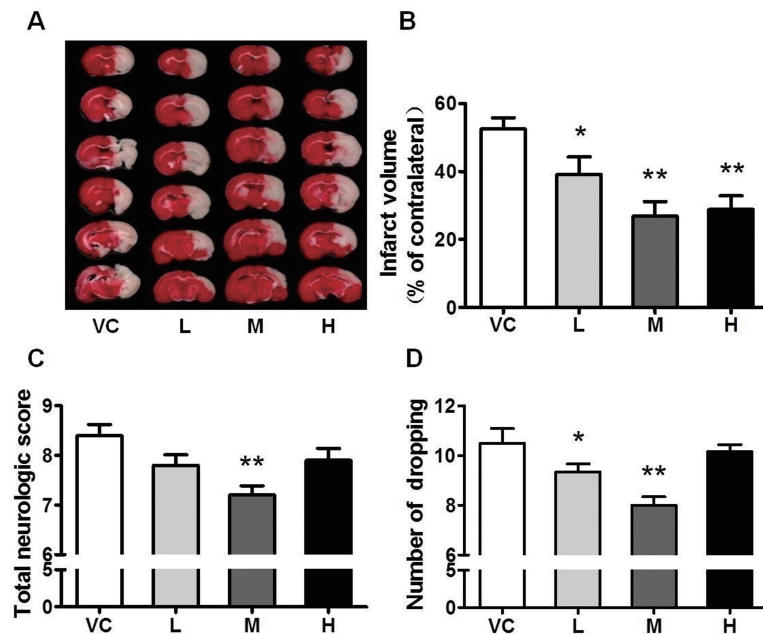
Figure 1. MB reduces the infarct volume and improves neurological functions. (A) Representative images of TTC-stained brain sections from the vehicle- or MB-treated animals collected 24 h after infarction. VC indicates vehicle control; and L, M and H represent low (1 mg/kg), medium (5 mg/kg) and high (10 mg/kg) dose MB, respectively. (B) Quantitative analysis of the infarct volume. (C) Total neurological deficit score. The medium dose of MB significantly attenuated the injury to the impaired forelimb. (D) Grid-walking test. The number of foot faults by the animals was significantly reduced by the low or medium dose of MB. n = 18-20; *$P < 0.05$, **$P < 0.01$ compared with the VC.

Figure 2. MB impedes the destruction of brain tissue. Brain sections were collected at 24 h after stroke. (A) Representative H&E staining in the cortex. The arrows indicate swelling cells. VC indicates vehicle control; and L, M and H, represent low, medium and high dose of MB, respectively. (B) Quantification the swelling cells. The percentage of the swelling cells was calculated as follows: swelling cells (%) = (the number of swelling cells/the total number of cells) × 100. MB obviously decreased the swelling cells caused by acute ischemia. n = 10; **$P < 0.01$ compared with the VC. Scale bar, 50 μm.

same time, we noticed that in this ischemia condition necrosis is the dominant cause of ischemic injury.
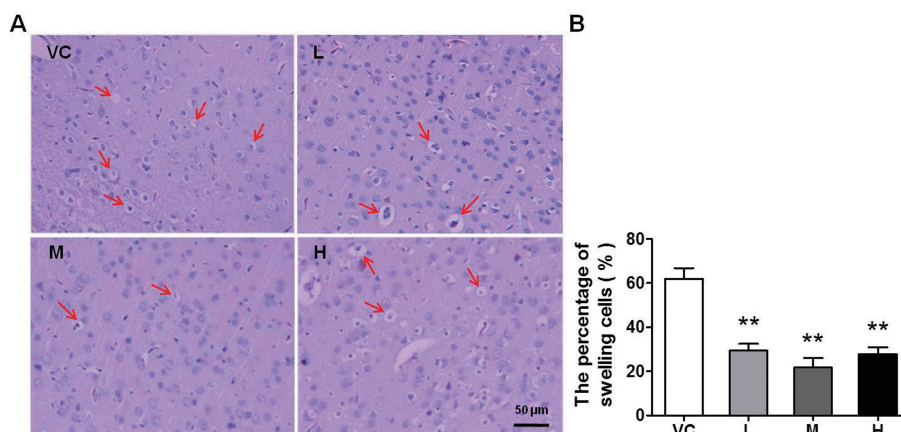
RIP1 and RIP3 are the key signaling molecules in programmed necrosis (44,45). To verify the effects of MB on necrosis, we measured the protein levels of RIP1 and RIP3 via Western blot. Compared to the contralateral (uninjured) side, ischemia (in the affected side) caused an elevation in the expression of both RIP1 and RIP3; however, MB suppressed this elevation of RIP1 and RIP3 expression (Figures 3D–F), suggesting a protective effect of MB against necrosis.

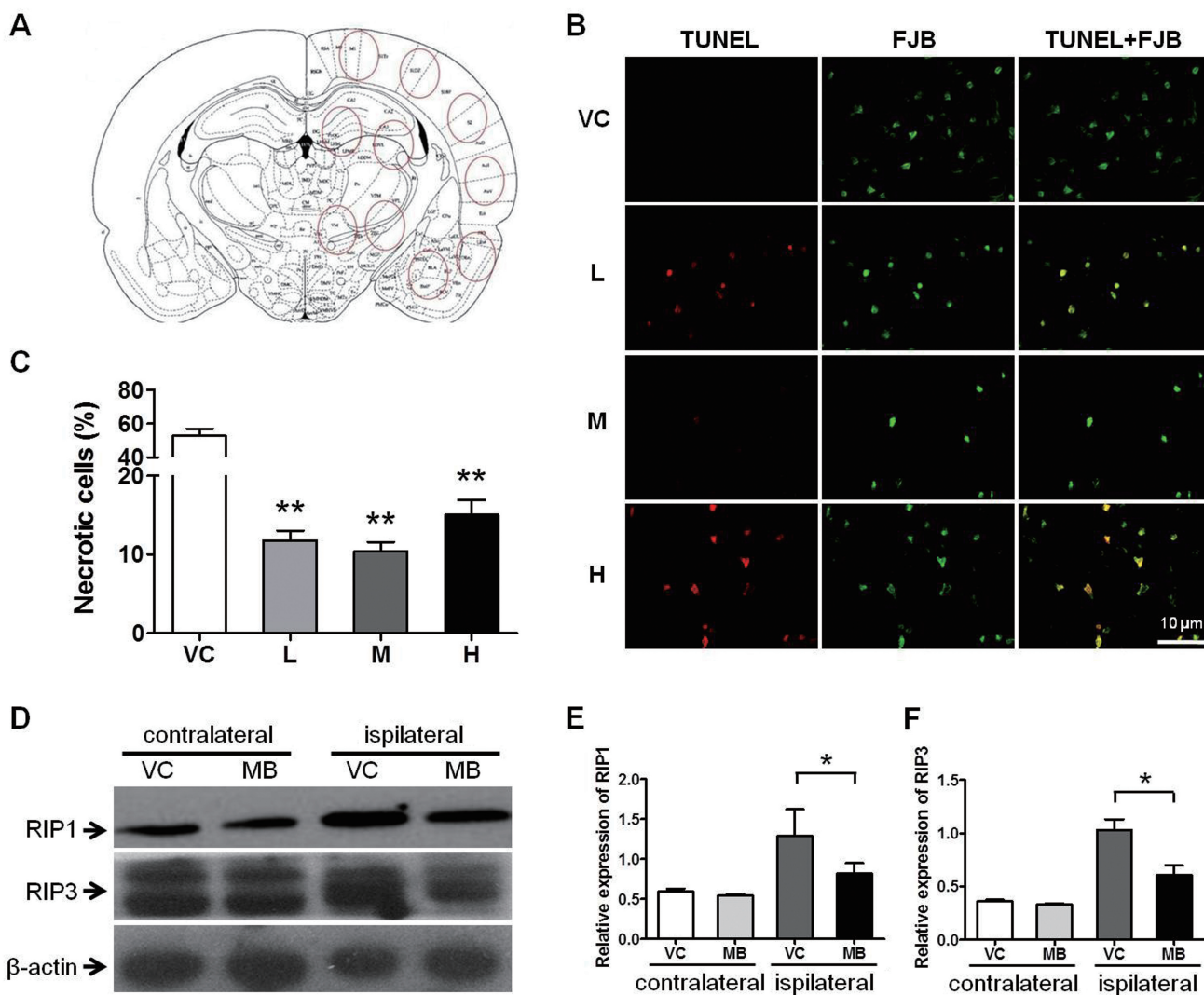## MB Improves the Structure of Mitochondria

The mitochondrion is a crucial target of MB. Whether the MB-mediated protection against ACI injury involves the regulation of mitochondria is unclear. Based on TEM, we found that the mitochondrial structures in the cortical neurons were severely damaged 24 h after stroke; the cristae were disrupted and disordered, the matrix granules were lost, and the mitochondria were vacuolated. All three doses of MB ameliorated the destruction of mitochondria (Figure 4A). The mitochondrial structure scoring data showed that the medium dose of MB exerted the most apparent effect (Figure 4B). The structure of mitochondria depends on the regulation of mitochondrial function. Mitophagy has an important function in clearance of the damaged mitochondria. Whether mitophagy is suppressed after stroke and whether MB is conductive to the induction of mitophagy need to be elucidated.

MB Increases the Induction of Mitophagy

The expression of Beclin-1, LC3, p62 and Tom20, which are molecular markers of mitophagy, was detected via Western blot. In the ipsilateral side of the VC group, the expression of Beclin-1 (representing the initiation of autophagy) and the flux of LC3 from I to II (suggesting the activation of autophagy)

Figure 3. MB alleviates necrosis. Necrosis was evaluated 24 h after stroke. (A) A schematic diagram of a coronal section of the brain. The red circles indicate the areas that we selected for imaging. (B) FJB and TUNEL double staining for the determination of necrosis. The FJB-labeled, TUNEL-negative cells are the necrotic cells. VC indicates vehicle control; and L, M and H, represent low, medium and high dose of MB, respectively. (C) Quantification of the percentage of necrotic cells. n = 25; **$P < 0.01$ compared with the VC. (D) Western blot analysis of the expression levels of the programmed necrosis molecules RIP1 and RIP3 from the brain tissue. β-actin was used as the internal control. The medium dose of MB was used in this assay. (E) and (F) The statistical analysis of the RIP1 and RIP3 expression levels. n = 5; *$P < 0.05$ compared with the VC in the ipsilateral hemisphere. Scale bar, 10 μm.

were reduced. p62 (an adaptor protein responsible for facilitating the binding of autophagic substrates to the autophagosome) and Tom20 (a mitochondrial outer membrane protein indicating the amount of mitochondria) were accumulated in the injured side compared with the contralateral side. Collectively, these results demonstrated that mitophagy was suppressed 24 h after

stroke. However, MB augmented mitophagy in both hemispheres, especially in the ipsilateral hemisphere, compared with the VC based on the increases in Beclin-1 expression and LC3 flux and the decreases in the p62 and Tom20 levels (Figures 5A, B). Based on TEM, the typical morphological characteristic of mitophagy, the encapsulation of a mitochondrion by the double membrane of

the autophagosome, was observed in the cortical neurons in the MB group, whereas a lack of mitophagy was observed in the VC group (Figure 5C). The mitochondrial ultrastructure further validated the mitophagy in the MB group. These results suggested that the augment of mitophagy by MB may contribute to the maintenance of mitochondrial quality following stroke.
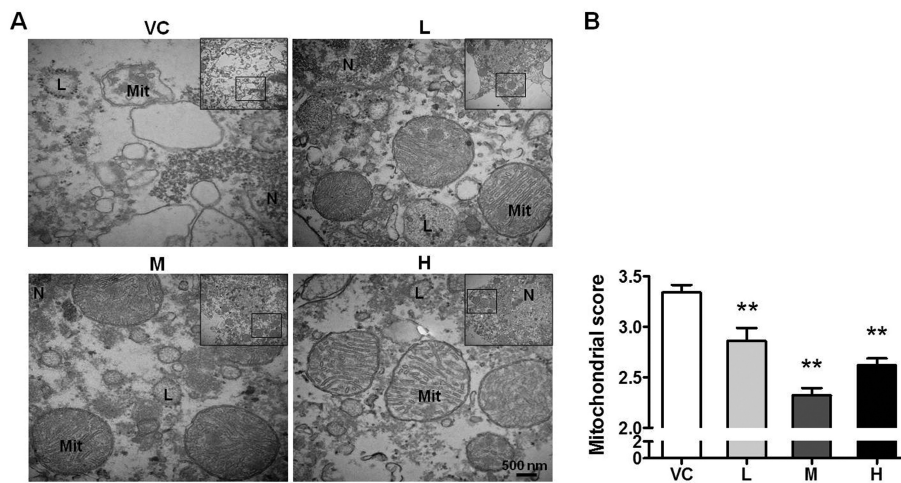
Figure 4. MB prevents the disruption of the mitochondrial structure. (A) The ultrastructure of mitochondria based on TEM. The box indicates the source of the high magnification image. Mit, mitochondria; N, nucleus; L, lysosome. VC indicates vehicle control; and L, M and H, represent low, medium and high dose of MB, respectively. (B) Quantification of the mitochondrial scores based on the integrality of mitochondrial structure. n = 20; **$P < 0.01$ compared with the VC. Scale bar, 500 nm.

Mitophagy Mediates the Protection of MB against Acute Ischemic Injury

To confirm whether mitophagy mediates the protective effect of MB against ACI injury, we first measured the effect of MB on mitophagy in an OGD model to simulate ACI injury *in vitro*. Figure 6A clearly displayed that after 2 h of OGD, MB promoted mitophagy as demonstrated by increased Beclin-1 expression and LC3 flux and decreased P62 and Tom20 levels. The statistical data show that 2 h of OGD induced mitophagy and MB dramatically enhanced the mitophagy under OGD (Figure 6B). Subsequently, we tested whether the protective effect of MB against ACI injury was altered after mitophagy was inhibited. Given that ROS are recognized as central mediators of neuroinflammation and cytotoxicity caused by ischemia and that mitophagy blocks the generation of ROS (24,46), we examined the ROS levels after mitophagy was inhibited. We found that OGD caused an elevation of ROS and that MB suppressed this elevation of ROS. As expected, when mitophagy was inhibited using 3-MA, an inhibitor of autophagy, the suppression of ROS accumulation by MB was abolished (Figures 6C, D). These results demonstrated that MB augmented the activity of mitophagy under OGD conditions, thereby mediating the reduction in the ROS levels.

## The MB-Induced Elevation of MMP Contributes to the Activation of Mitophagy

How did MB augment mitophagy in the case of ACI injury? Because mitophagy is directly induced by the loss of MMP (33,47), and because the reduction in MMP can be attenuated by MB (47), we analyzed the MMP via flow cytometry and measured mitophagy via Western blot in the OGD model. The MMP sharply fell after the cells were exposed to OGD for 2 h and MB significantly attenuated this decline, even though MB in the absence of OGD induced a decrease in the MMP (Figures 7A–B). To explore whether the elevation of MMP by MB under OGD conditions mediates the induction of mitophagy, we detected the change of mitophagy after the reduction in the MMP during OGD was further exacerbated via the addition of CCCP, a mitochondria-depolarizing agent. CCCP induced a sharp drop in the MMP, and MB greatly attenuated the decline in the

MMP (Supplementary Figure 2). After OGD treatment, mitophagy was inhibited, and MB augmented mitophagy as shown in Figure 5A; however, when the MMP was further reduced due to the addition of CCCP, the augmentation of mitophagy by MB was suppressed (Figure 7C). These results revealed that sustaining the MMP at a higher level using MB under OGD conditions contributed to the induction of mitophagy.

DISCUSSION

Stroke is the fourth leading disease that threatens human life and health (48). Acute cerebral ischemia is the primary cause of stroke. At present, there is a lack of effective drugs for the treatment of ACI injury. Another issue is that fewer than 5% of stroke patients can obtain thrombolytic therapy within the therapeutic window. Therefore, seeking effective neuroprotective drugs is an immediate focus. MB is a lipophilic compound that has been used for the treatment of multiple disorders, including methemoglobinemia, malaria and cyanide poisoning (9,10,49). Recently, MB has been shown to play neuroprotective roles in a variety of mitochondria-associated cytotoxicity paradigms, such as stroke, Parkinson's disease, Alzheimer's disease, Huntington's disease and optic neuropathy (30,47). In this study, we demonstrated for the first time that MB attenuates ACI injury by increasing the induction of mitophagy.

We have identified that MB reduces the infarct volume and the neurological dysfunction caused by ACI injury. To investigate the impact of MB on brain tissue structure after stroke, we observed the changes in cell morphology. Cell swelling and nuclear pyknosis were reduced due to MB treatment. Based on further analysis of apoptosis and necrosis, we determined the role of MB in ameliorating necrosis. We were also surprised to find that MB did not decrease but rather increased apoptosis. The reason for this increase in apoptosis appears to be related to its reduction of necrosis, representing a compromise mechanism
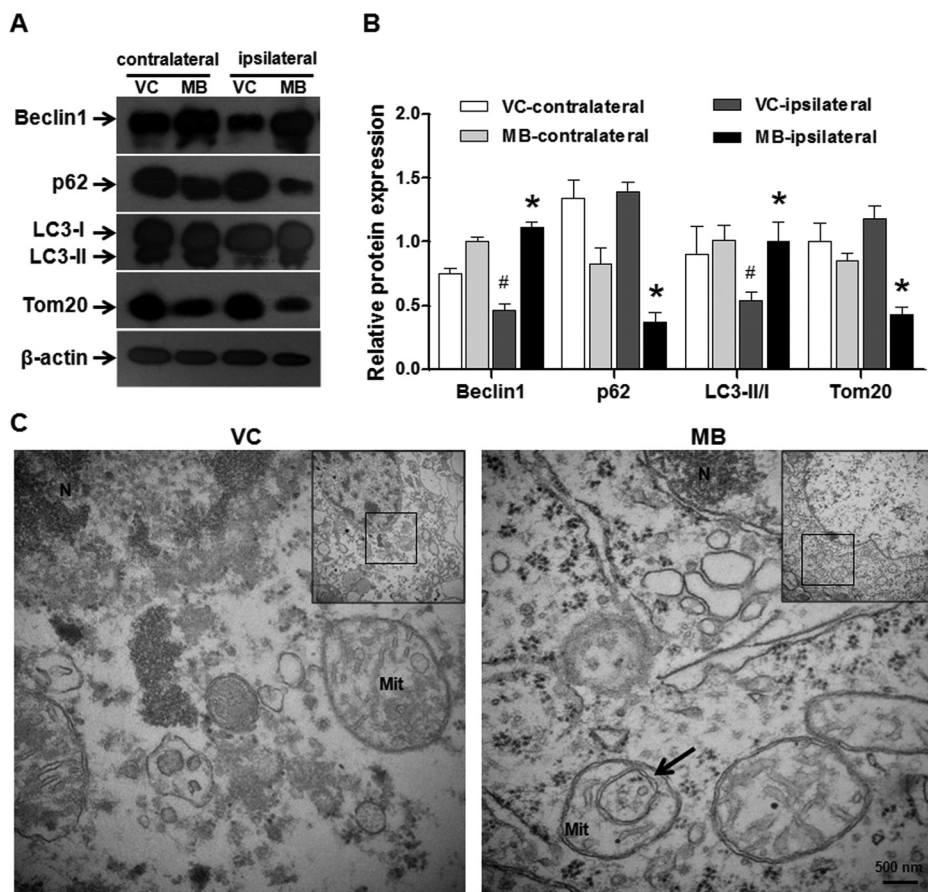
Figure 5. MB increases the induction of mitophagy. (A) Western blot analysis of mitophagy. β-actin was used as the internal control. The medium dose of MB (5 mg/kg) was used in this assay. Mitophagy was augmented by the MB treatment. (B) The statistical analysis of mitophagy levels. n = 5; *$P < 0.05$ compared with the VC in the ipsilateral hemisphere, #$P < 0.05$ compared with the VC in the contralateral hemisphere. (C) TEM-based determination of mitophagy. The arrow indicates a mitochondrion encapsulated by the double membrane of an autophagosome. The typical structure of mitophagy verified the effect of MB on mitophagy after stroke. Scale bar, 500 nm.

that avoids additional necrosis in stroke. The expression of key signaling molecules in programmed necrosis, RIP1 and RIP3 was decreased significantly by MB, suggesting the suppression of necrotic activity. Collectively, these results supported that hindering the necrotic process contributes to the protective effect of MB against ACI injury.

To identify the potential mechanism by which MB inhibited necrosis, we focused on the effect of MB on mitochondrial structure and function after stroke, considering that the mitochondrion is an important target of MB (50). The observa-

tion and scoring of the mitochondrial ultrastructure indicated that the mitochondrial structure was seriously disrupted after stroke, but that MB dramatically ameliorated the disintegration of the mitochondrial structure. This result inspired us to explore whether mitochondrial function was also improved by MB in stroke. Mitophagy functions as selective clearance of damaged mitochondria to reduce necrosis or apoptosis and to sustain cellular activity (31,51). Therefore, mitophagy is considered as a protective response to a variety of stresses. At 24 h after ACI, mitophagy was sup-

pressed to a large extent. However, to our excitement, mitophagy was clearly augmented by MB treatment compared with the VC treatment. Thus, the augmentation of mitophagy may at least partially explain the maintenance of the mitochondrial structure by MB in stroke. To further verify whether mitophagy mediated the protective effect of MB against ACI injury, we examined the ROS levels in an OGD model *in vitro*. We found that OGD caused a dramatic elevation of ROS, MB greatly suppressed this elevation, and the suppression of MB was abolished after mitophagy was inhibited, demonstrating that mitophagy mediates the protective effect of MB against ACI injury.

MMP is an electrostatic potential generated by the proton gradient across the mitochondrial inner membrane that is driven by the enzymes of electron transport chain (ETC). The MMP is an indicator of the mitochondrial functional status, and deregulation of MMP leads to a large spectrum of major human diseases, including diabetes, neurodegeneration, cancer and others (52). It has been reported that MB maintains the MMP when mitochondria are dysfunctional (2), and the MMP is a regulator of mitophagy (27). Accordingly, we investigated the effect of MB on the MMP and the relationship between the MMP and the induction of mitophagy. We discovered that the dramatic decline in the MMP under OGD conditions was greatly hindered by MB, and unexpectedly, MB in the absence of OGD induced a decrease in the MMP. Based on MB's redox properties that low MB concentrations favor dimerization and reduction, whereas high concentrations promote oxidation (7), we propose the following hypothesis for this phenomenon: in functional mitochondria, MB in its reduced form donates H^+ (47), which tends to cause an elevation of MMP; MB in its oxidized form accepts H^+ (53), which tends to cause a decline of MMP. However, in dysfunctional mitochondria, these effects may be just opposite. When the activities of ETC enzymes are decreased, MMP
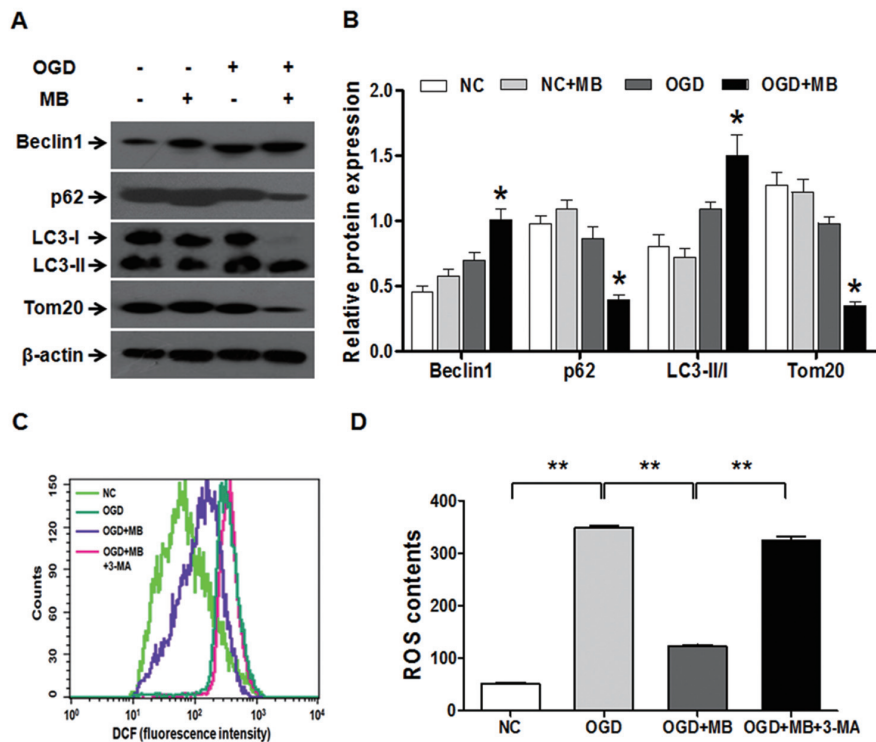
Figure 6. Mitophagy mediates the protective effect of MB against acute ischemic injury *in vitro*. (A) Mitophagy is augmented by MB (0.5 μmol/L) under OGD conditions as evaluated by Western blot. β-actin was used as the internal control. NC, normal control; OGD, oxygen-glucose deprivation. (B) The statistical analysis of mitophagy levels. n = 4; *P < 0.05 compared with the OGD group. (C) The ROS levels were reduced by 0.5 μmol/L MB but were restored by the addition of 3-MA (2 mmol/L), an inhibitor of autophagy. The inhibition of mitophagy using 3-MA increased the generation of ROS during OGD and abolished the protective effect of MB. (D) Quantitative analysis of the contents of ROS. n = 4; **P < 0.01, *P < 0.05 between the indicated groups.

drops rapidly and excessive H^+ in the mitochondrial matrix provided by MB in its reduced form cannot be pumped out into the mitochondrial intermembrane space, which aggravates the drop of MMP; in contrast, MB in its oxidized form can accept the H^+ that cannot be pumped out due to the decreased activities of ETC enzymes, which hinders the further drop of MMP. It thus seems that 0.5 μmol/L MB we used in this study displayed its oxidation properties. That is, it decreased the MMP in the normal conditions and attenuated the drop of MMP in the OGD conditions. Furthermore, we demonstrated that the augment of mitophagy by MB was completely abolished due to the addition of CCCP. These results suggested that the maintenance of MMP by MB in stroke promoted the induction of mitophagy.

CONCLUSION

In summary, our study demonstrated that the suppression of mitophagy is involved in the pathogenesis of stroke. More importantly, we confirmed that the augmentation of mitophagy by MB mediates the protection against ACI injury. Thus, we propose that MB is a promising neuroprotective agent against acute ischemic stroke.
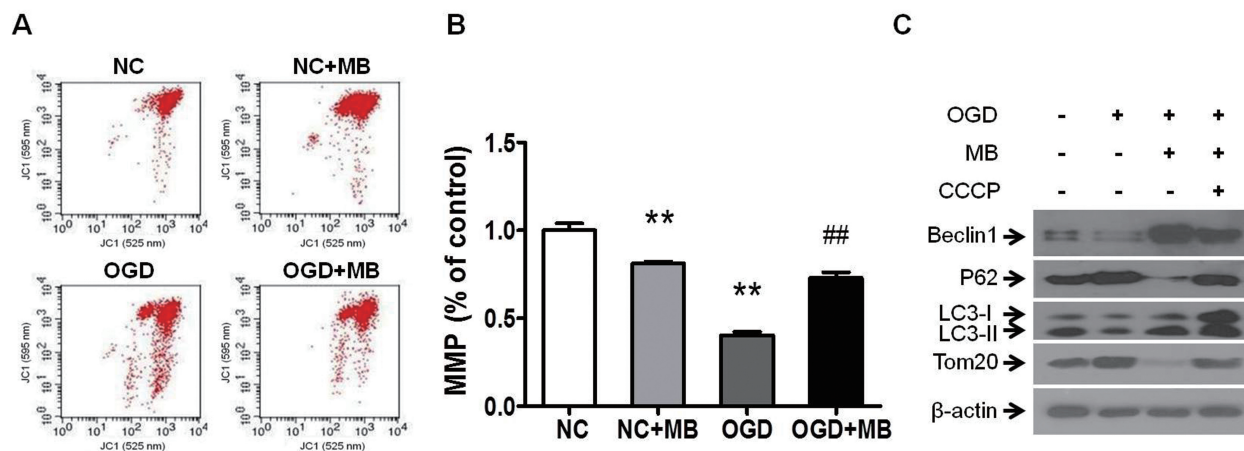
Figure 7. The MB-mediated elevation of the MMP under OGD conditions contributes to the activation of mitophagy. (A) MB (0.5 μmol/L) alleviates the decline in the MMP during OGD based on flow cytometric analysis. (B) Quantification of the MMP. n = 4; **P < 0.01 compared with the NC, ##P < 0.01 compared with OGD. (C) Western blot analysis of mitophagy. β-actin was used as the internal control. Exacerbating the decline in the MMP with CCCP (1 μmol/L) abolishes the induction of mitophagy by MB.

ACKNOWLEDGMENTS

DISCLOSURE

The authors declare that they have no competing interests as defined by *Molecular Medicine*, or other interests that might be perceived to influence the results and discussion reported in this paper.

REFERENCES

1. Wainwright M, Crossley KB. (2002) Methylene Blue - a therapeutic dye for all seasons? *J. Chemother.* 14:431–43.
2. Tretter L, Horvath G, Holgyesi A, Essek F, Adam-Vizi V. (2014) Enhanced hydrogen peroxide generation accompanies the beneficial bioenergetic effects of methylene blue in isolated brain mitochondria. *Free Radic. Biol. Med.* 77:317–30.
3. Oz M, Lorke DE, Hasan M, Petroianu GA. (2011) Cellular and molecular actions of Methylene Blue in the nervous system. *Med. Res. Rev.* 31:93–117.
4. Callaway NL, Riha PD, Bruchey AK, Munshi Z, Gonzalez-Lima F. (2004) Methylene blue improves brain oxidative metabolism and memory retention in rats. *Pharmacol. Biochem. Behav.* 77:175–81.
5. Zhang X, Rojas JC, Gonzalez-Lima F. (2006) Methylene blue prevents neurodegeneration caused by rotenone in the retina. *Neurotox. Res.* 9:47–57.
6. Riha PD, Bruchey AK, Echevarria DJ, Gonzalez-Lima F. (2005) Memory facilitation by methylene blue: dose-dependent effect on behavior and brain oxygen consumption. *Eur. J. Pharmacol.* 511:151–8.
7. Rojas JC, Bruchey AK, Gonzalez-Lima F. (2012) Neurometabolic mechanisms for memory enhancement and neuroprotection of methylene blue. *Prog. Neurobiol.* 96:32–45.
8. Kelner MJ, Bagnell R, Hale B, Alexander NM. (1988) Potential of methylene blue to block oxygen radical generation in reperfusion injury. *Basic Life Sci.* 49:895–8.
9. Cawein M, Behlen CH 2nd, Lappat EJ, Cohn JE. (1964) Hereditary diaphorase deficiency and methemoglobinemia. *Arch Intern Med* 113:578–85.
10. Draize JH. (1933) Sodium tetrathionate and methylene blue in cyanide and carbon monoxide poisoning. *Science.* 78:145.
11. Wen Y, *et al.* (2011) Alternative mitochondrial electron transfer as a novel strategy for neuroprotection. *J. Biol. Chem.* 286:16504–15.
12. Miclescu A, Sharma HS, Martijn C, Wiklund L. (2010) Methylene blue protects the cortical blood-brain barrier against ischemia/reperfusion-induced disruptions. *Crit. Care Med.* 38:2199–206.
13. Shen Q, *et al.* (2013) Neuroprotective efficacy of methylene blue in ischemic stroke: an MRI study. *PLoS One.* 8:e79833.
14. Gropen TI, *et al.* (2006) Quality improvement in acute stroke: the New York State Stroke Center Designation Project. *Neurology.* 67:88–93.
15. Ertracht O, Malka A, Atar S, Binah O. (2014) The mitochondria as a target for cardioprotection in acute myocardial ischemia. *Pharmacol. Ther.* 142:33–40.
16. Kim SY, *et al.* (2014) Inhibition of cyclophilin D by cyclosporin A promotes retinal ganglion cell survival by preventing mitochondrial alteration in ischemic injury. *Cell Death Dis.* 5:e1105.
17. Ikeda Y, *et al.* (2015) Endogenous drp1 mediates mitochondrial autophagy and protects the heart against energy stress. *Circ. Res.* 116:264–78.
18. Lemasters JJ. (2005) Selective mitochondrial autophagy, or mitophagy, as a targeted defense against oxidative stress, mitochondrial dysfunction, and aging. *Rejuvenation Res.* 8:3–5.
19. Youle RJ, Narendra DP. (2011) Mechanisms of mitophagy. *Nat. Rev. Mol. Cell Biol.* 12:9–14.
20. Ashrafi G, Schlehe JS, LaVoie MJ, Schwarz TL. (2014) Mitophagy of damaged mitochondria occurs locally in distal neuronal axons and requires PINK1 and Parkin. *J. Cell Biol.* 206:655–70.
21. Liu L, *et al.* (2012) Mitochondrial outer-membrane protein FUNDC1 mediates hypoxia-induced mitophagy in mammalian cells. *Nat. Cell Biol.* 14:177–85.
22. Kim I, Lemasters JJ. (2011) Mitophagy selectively degrades individual damaged mitochondria after photoirradiation. *Antioxid. Redox. Signal.* 14:1919–28.
23. Wu H, *et al.* (2014) The BCL2L1 and PGAM5 axis defines hypoxia-induced receptor-mediated mitophagy. *Autophagy.* 10:1712–25.
24. Kurihara Y, *et al.* (2012) Mitophagy plays an essential role in reducing mitochondrial production of reactive oxygen species and mutation of mitochondrial DNA by maintaining mitochondrial quantity and quality in yeast. *J. Biol. Chem.* 287:3265–72.
25. Bin-Umer MA, McLaughlin JE, Butterly MS, McCormick S, Tumer NE. (2014) Elimination of damaged mitochondria through mitophagy reduces mitochondrial oxidative stress and increases tolerance to trichothecenes. *Proc. Natl. Acad. Sci. U. S. A.* 111:11798–803.
26. Schapira AH, Olanow CW, Greenamyre JT, Bezard E. (2014) Slowing of neurodegeneration in Parkinson's disease and Huntington's disease: future therapeutic perspectives. *Lancet* 384:545–55.
27. Shiba-Fukushima K, *et al.* (2014) Phosphorylation of mitochondrial polyubiquitin by PINK1 promotes parkin mitochondrial tethering. *PLoS. Genet.* 10:e1004861.
28. Santos RX, *et al.* (2011) Mitophagy in neurodegeneration: an opportunity for therapy? *Curr. Drug Targets.* 12:790–9.
29. Rubinsztein DC, Marino G, Kroemer G. (2011) Autophagy and aging. *Cell.* 146:682–95.
30. Martinez-Vicente M, *et al.* (2010) Cargo recognition failure is responsible for inefficient autophagy in Huntington's disease. *Nat. Neurosci.* 13:567–76.
31. Lemasters JJ, *et al.* (1998) The mitochondrial permeability transition in cell death: a common mechanism in necrosis, apoptosis and autophagy. *Biochim. Biophys. Acta.* 1366:177–96.
32. Hollville E, Carroll RG, Cullen SP, Martin SJ. (2014) Bcl-2 family proteins participate in mitochondrial quality control by regulating Parkin/PINK1-dependent mitophagy. *Mol. Cell.* 55:451–66.
33. Strappazzon F, *et al.* (2015) AMBRA1 is able to induce mitophagy via LC3 binding, regardless of PARKIN and p62/SQSTM1. *Cell Death Differ.* 22:419–32.
34. Zhang JH, *et al.* (2015) 5-HMF prevents against oxidative injury via APE/Ref-1. *Free Radic. Res.* 49:86–94.
35. Belayev L, Alonso OF, Busto R, Zhao W, Ginsberg MD. (1996) Middle cerebral artery occlusion in the rat by intraluminal suture. Neurological and pathological evaluation of an improved model. *Stroke.* 27:1616–22; discussion 1623.
36. Baskin YK, Dietrich WD, Green EJ. (2003) Two effective behavioral tasks for evaluating sensori-motor dysfunction following traumatic brain injury in mice. *J. Neurosci. Methods.* 129:87–93.
37. Lin TN, He YY, Wu G, Khan M, Hsu CY. (1993) Effect of brain edema on infarct volume in a focal cerebral ischemia model in rats. *Stroke* 24:117–21.
38. Liu H, *et al.* (2015) Targeting heat-shock protein 90 with ganetespib for molecularly targeted therapy of gastric cancer. *Cell Death Dis.* 6:e1595.
39. Back SA, *et al.* (2007) Hypoxia-ischemia preferentially triggers glutamate depletion from oligodendroglia and axons in perinatal cerebral white matter. *J. Cereb. Blood Flow Metab.* 27:334–47.
40. Flameng W, Borgers M, Daenen W, Stalpaert G. (1980) Ultrastructural and cytochemical correlates of myocardial protection by cardiac hypothermia in man. *J. Thorac. Cardiovasc. Surg.* 79:413–24.
41. Li Y, *et al.* (2011) Spatiotemporal pattern of neuronal injury induced by DFP in rats: a model for delayed neuronal cell death following acute OP intoxication. *Toxicol. Appl. Pharmacol.* 253:261–9.

42. Cheng X, *et al*. (2014) A TrxR inhibiting gold(I) NHC complex induces apoptosis through ASK1-p38-MAPK signaling in pancreatic cancer cells. *Mol. Cancer*. 13:221.

43. Moskowitz MA, Lo EH, Iadecola C. (2010) The science of stroke: mechanisms in search of treatments. *Neuron*. 67:181–98.

44. Narayan N, *et al*. (2012) The NAD-dependent deacetylase SIRT2 is required for programmed necrosis. *Nature*. 492:199–204.

45. Wang Z, Jiang H, Chen S, Du F, Wang X. (2012) The mitochondrial phosphatase PGAM5 functions at the convergence point of multiple necrotic death pathways. *Cell*. 148:228–43.

46. Singhal A, Morris VB, Labhasetwar V, Ghorpade A. (2013) Nanoparticle-mediated catalase delivery protects human neurons from oxidative stress. *Cell Death Dis*. 4:e903.

47. Poteet E, *et al*. (2012) Neuroprotective actions of methylene blue and its derivatives. *PLoS One*. 7:e48279.

48. Lopez-Valdes HE, *et al*. (2014) Memantine enhances recovery from stroke. *Stroke*. 45:2093–100.

49. Coulibaly B, *et al*. (2015) Efficacy and safety of triple combination therapy with artesunate-amodiaquine-methylene blue for falciparum malaria in children: a randomized controlled trial in burkina faso. *J. Infect. Dis*. 211:689–697.

50. Congdon EE, *et al*. (2012) Methylthioninium chloride (methylene blue) induces autophagy and attenuates tauopathy in vitro and in vivo. *Autophagy*. 8:609–22.

51. Kubli DA, Gustafsson AB. (2012) Mitochondria and mitophagy: the yin and yang of cell death control. *Circ. Res*. 111:1208–21.

52. Bagkos G, Koufopoulos K, Piperi C. (2014) A new model for mitochondrial membrane potential production and storage. *Med. Hypotheses*. 83:175–81.

53. Gabrielli D, Belisle E, Severino D, Kowaltowski AJ, Baptista MS. (2004) Binding, aggregation and photochemical properties of methylene blue in mitochondrial suspensions. *Photochem. Photobiol*. 79:227–32.